Received: 10 February 2022 | Revised: 2 September 2022 | Accepted: 5 September 2022

DOI: 10.1111/fog.12612

ORIGINAL ARTICLE

FISHERIES OCEANOGRAPHY WILEY

NPFC-2022-SSC BFME03-IP03

Effects of oceanography on North Pacific armorhead recruitment in the Emperor Seamounts

Madeline A. K. Lavery[1,2] | Christopher N. Rooper[1] | Kota Sowada[3] | Kari Fenske[4] | Vladimir Kulik[5] | Kyum Joon Park[6]

[1]Stock Assessment and Research Division, Pacific Biological Station, Fisheries and Oceans Canada, Nanaimo, British Colombia, Canada

[2]Department of Biology, University of Victoria, Victoria, British Colombia, Canada

[3]Oceanic Resources Group, Highly Migratory Resources Division, Fisheries Stock Assessment Center, Fisheries Resources Institute, Japan Fisheries Research and Education Agency, Yokohama, Kanagawa, Japan

[4]Wisconsin Department of Natural Resources, Madison, Wisconsin, USA

[5]Pacific Branch (TINRO), Russian Federal Research Institute Of Fisheries and Oceanography (VNIRO), Vladivostok, Primorsky Krai, Russia

[6]National Institute of Fisheries Science, Ministry of Ocean and Fisheries, Busan, South Korea

Correspondence
Madeline A. K. Lavery, Stock Assessment and Research Division, Pacific Biological Station, Fisheries and Oceans Canada, 31900 Hammond Bay Road, Nanaimo, British Colombia V9T 6N7, Canada.
Email: madeline.lavery@dfo-mpo.gc.ca

Abstract

The North Pacific armorhead (NPA), *Pentaceros wheeleri*, is thought to exhibit an extended post-spawning epipelagic phase in which larvae disperse to the northeast Pacific Ocean. Current understanding of juvenile distribution, development, and mechanisms that drive recruitment variation, however, remains largely incomplete. The objective of this study was to compare a time series of NPA recruitment to established climate indices and to environmental covariates to explore drivers of the NPA life cycle. Additionally, this work investigates potential larval NPA transport pathways and their positional relationships to the proposed northeastern nursery grounds. Using Lagrangian particle tracking, trajectories of passive larvae were simulated at depths of 0 and 15 m for 18 years (2001–2018) from the Southern Emperor-Northern Hawaiian Ridge (SE-NHR) natal habitat. Dispersal distances and particle end positions were examined for their potential relationships with recruitment. Sea surface temperature and net primary productivity were evaluated as predictor variables using generalized additive modeling. Neither regression of particle end-point characteristics nor environmental covariates resulted in significant correlations with recruitment here, perhaps owing to data limitations surrounding the nursery zone. Particles were found to be advected largely within the North Pacific transition zone in the central north Pacific. Significant seasonal correlations were found between recruitment and the Arctic Oscillation, Pacific Decadal Oscillation and North Pacific Gyre Oscillation, suggesting that NPA recruitment mechanisms respond to interannual ocean-atmospheric climate oscillations. Better knowledge of the connections between recruitment and the environment would be valuable for stock management, and improvements for advection predictions are discussed.

KEYWORDS
climate effects, environmental covariates, North Pacific armorhead, oceanography, OceanParcels, recruitment

1 | INTRODUCTION

Since the late 1960s, North Pacific armorhead (NPA) have experienced intense bottom-trawl fishing pressure in the central North Pacific. Commercial over-exploitation was immediate following the rise of a groundfish fishery at the largest concentration of demersal NPA over the Southern Emperor-Northern Hawaiian Ridge (SE-NHR) seamounts, and fishing effort then spread throughout the Hawaiian archipelago (Uchida & Tagami, 1984). Catch of NPA significantly declined in 1977 and has since remained at extremely low levels

(Kiyota et al., 2016). The current NPA fishery, which occurs in international waters and is managed by the North Pacific Fisheries Commission (NPFC; a Regional Fisheries Management Organization), is generally sustained by intermittent recruitment events occurring every 5–10 years (NPFC, 2021).

NPA remain at-present a data-poor species (Kiyota et al., 2016). The NPA life cycle consists of an extended epipelagic phase of approximately 1.5–2.5 years, followed by a transition into the demersal zone in later life stages (Boehlert & Sasaki, 1988). Spawning occurs over winter between November and March and is believed to occur solely at the SE-NHR seamounts, shown in Figure 1 (Kiyota et al., 2016). For the first several months after spawning occurs, eggs and larvae are neustonic and are either advected in wind-driven currents or actively move northeastward (Boehlert & Sasaki, 1988; Humphreys et al., 1993). Juveniles feed and grow steadily in the northeastern subarctic Pacific, which is hypothesized to provide a suitable nursery ground habitat (Humphreys et al., 1993; Murakami et al., 2016). At some point during their pelagic phase, NPA develop a capacity to swim actively and have been suggested to exhibit schooling behavior based on presence of aggregated samples in sei whale stomach content analyses (Boehlert & Sasaki, 1988; Chikuni, 1970). Following the pelagic phase, sub-adults return to the SE-NHR seamounts, where recruitment to the adult stock is estimated to occur principally in late spring to summer (Humphreys et al., 1989, 1993; Kiyota et al., 2016). NPA recruitment strength has been historically highly sporadic, producing significant interannual fluctuations in this species' biomass.

Given the prevalence of variable recruitment strength among many fish species, recruitment studies in recent years have sought to investigate physical and biological driving sources of recruitment variability using multidisciplinary modeling strategies in order to incorporate these factors into management (Houde, 2008; Ludsin et al., 2014; Wilson et al., 2008). Local surface environmental conditions such as sea surface temperature (SST) and food availability are driven by interactions between oceanographic features, geographical morphology, and weather effects (Keyl & Wolff, 2008) and have significant influences on fish survival (Pécuchet et al., 2015). Physical transport of larvae is another principal determinant of year-class strength, as fish commonly rely on current transport during larval stages for dispersal to nursery zone systems (Norcross & Shaw, 1984). Ocean circulation patterns, eddy dynamics, and fronts, such as those that occur within the North Pacific transition zone, are therefore often found to relate to pelagic species' larval distributions, as well as to migration and foraging patterns in later life stages (Laurs & Lynn, 1977; Pattrick et al., 2021; Polovina et al., 2001; Sánchez-Velasco et al., 2013; Wolanki & Hamner, 1988). Early NPA survival success theories have suggested that thermal and prey associations are likely important, while other research has shown that transport of NPA eggs and larvae to unfavorable regions during the pelagic phase due to interannual surface current variations could be a determinant of year-class strength (Boehlert & Sasaki, 1988). Relating the physical environment to recruitment is in itself a profoundly difficult endeavor, as the environment varies spatially and temporally, and biological responses are complex and occur at various scales.

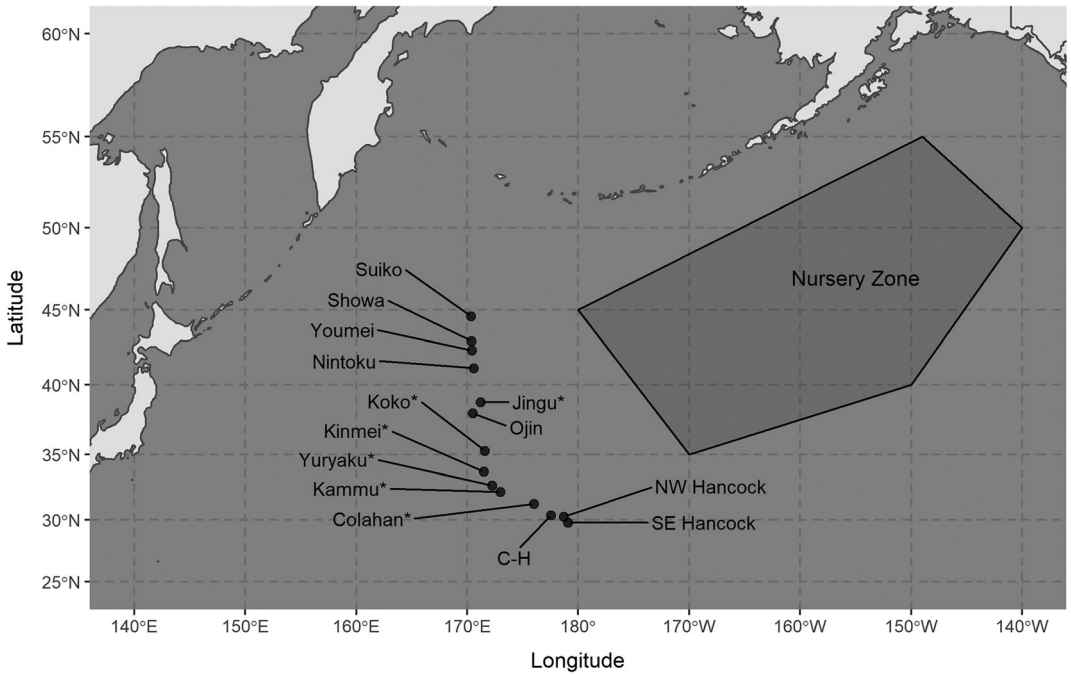

FIGURE 1 Map of the northeast Pacific showing potential Southern Emperor-Northern Hawaiian Ridge natal seamounts of NPA (black circles) and the nursery zone polygon employed in this study. Six central seamounts (denoted with an asterisk) were selected as the OceanParcels simulation particle release locations.

Large-scale climate indices, which act as proxies for coupled atmosphere–ocean processes that drive climatic variability (Litzow et al., 2020), are commonly compared with recruitment data and can be valuable in detecting drivers of fish stock abundance changes. The Pacific Decadal Oscillation (PDO) and the North Pacific Gyre Oscillation (NPGO) climate indices are, respectively, defined as the leading principal component of SST variability in the North Pacific (Mantua et al., 1997) and the second principal component of variability in sea surface height anomalies (Di Lorenzo et al., 2008). The PDO and NPGO indices have been demonstrated to correlate on interannual time scales to regional environmental conditions in the northeast Pacific (Litzow et al., 2018), as well as to marine life fluctuations throughout the Pacific Ocean (Chavez et al., 2003; Chhak et al., 2009; Coffin & Mueter, 2016; Johnson et al., 2020; Lee et al., 2009; Mantua & Hare, 2002). Other indices, including the Arctic Oscillation (AO), the North Pacific Index (NPI), and the Aleutian Low Pressure Index (ALPI; Rodionov et al., 2007), have been demonstrated to couple with marine production (Beamish & Bouillon, 1993; Schwing et al., 2003). While connections between NPA recruitment and their environment continue to be mainly unresolved due to this species' data limitations, a previous analysis that simulated NPA larval dispersal observed a negative relationship between catch and the PDO index (Yonezaki et al., 2017), suggesting that correlations between climate datasets and NPA may exist.

As the information currently available for managing the NPA fishery is limited, further insight into recruitment processes for NPA is crucial for maintenance of both the species and the fishery. An improved understanding of the effects of large-scale atmospheric and oceanic conditions on NPA recruitment would aid in their assessment and sustainable harvesting based on the precautionary principles outlined by NPFC regulations. This study aims to (1) examine the relationship between NPA recruitment and large-scale and local oceanographic conditions; (2) investigate egg and larval transport pathways using a Lagrangian particle tracking approach; and (3) examine the proposed nursery zone in the northeast Pacific in relation to simulated end positions of advected particles. We hypothesize that recruitment may be correlated to basin-scale conditions in the North Pacific. In particular, elevated SSTs and higher levels of productivity may show a positive relationship with recruitment strength, and advection or retention patterns of drifting eggs and larvae may have a significant effect on recruitment.

2 | METHODS

2.1 | Study area

The SE–NHR is a chain of volcanic submarine seamounts in the central North Pacific Ocean, spanning from 32°N to 53°N in the region of 170°E. The seamounts of the SE-NHR have irregular shapes and span from 50 to 100 km wide (Roden, 1984). The seamounts interact with the flow of the Kuroshio Extension and the Subarctic Current (Figure 2), producing variable water current features, as well as upwelling and downwelling patterns based on individual seamount topographies (Roden, 1984). Larger seamounts, including Kammu, Yuryaku, and Koko, may produce more complex current-topography

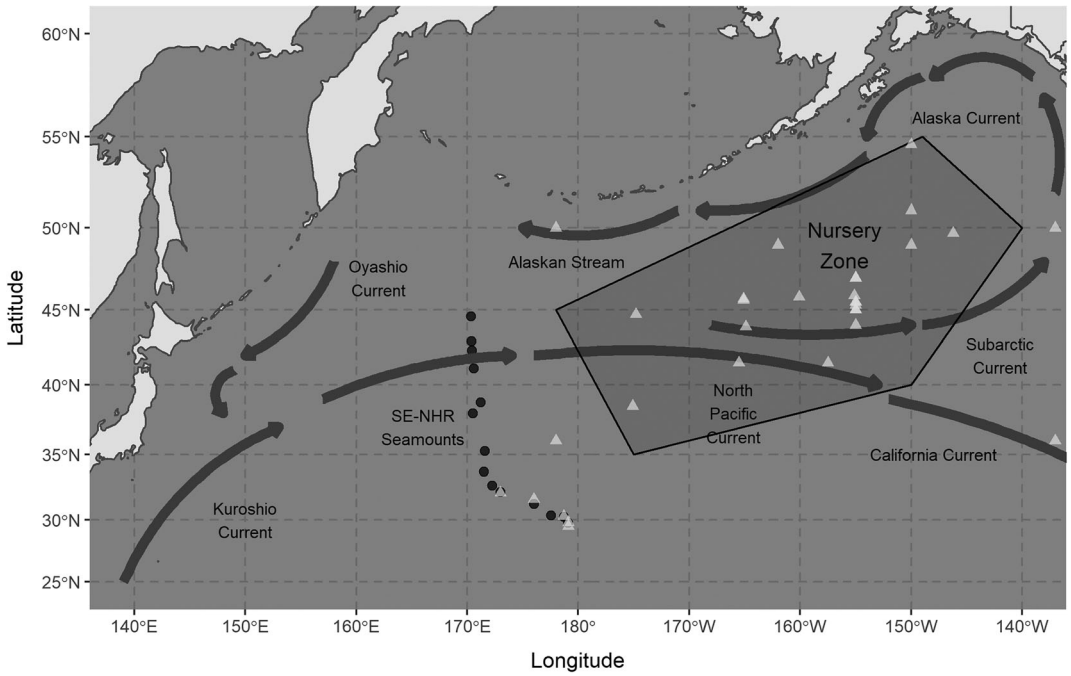

FIGURE 2 Map of the northeast Pacific showing the potential Southern Emperor-Northern Hawaiian Ridge seamounts (black circles), flow directions of major North Pacific currents (gray arrows), the nursery zone used in this study (gray polygon), and previous occurrences of NPA (white triangle points) described by Boehlert and Sasaki (1988), Murakami et al. (2016), Humphreys et al. (1993), and Humphreys (2000)

effects such as recirculation and increased retention of organisms in contrast to small-summited guyot-type seamounts such as Colahan (Boehlert et al., 1994; Humphreys, 2008).

The North Pacific Fisheries Commission (NPFC) bottom fisheries 2021 footprint document (www.npfc.int/statistics) summarizes fishing activity at 14 of the SE-NHR seamounts, shown in Figure 1. The highest relative abundance of NPA at the SE-NHR is suggested to occur near the central seamounts Colahan, C-H, and Hancock (Uchida & Tagami, 1984). Six seamounts between 31.3°N and 38.8°N and 171.2°E and 176°E; Jingu, Koko, Kinmei, Yuryaku, Kammu, and Colahan, were selected for use in our study based on the suggested center of abundance of NPA. Deeper-summited SE-NHR seamounts north of 35°N and seamounts closer to the Hawaiian ridge are not expected to be used by NPA (Uchida & Tagami, 1984) and thus were excluded as spawning sites. Juvenile NPA have been recorded widely throughout the central and east North Pacific Ocean, therefore the simulation study area extended across the North Pacific Ocean between 25°N to 62°N and 130°E to 120°W.

2.2 | Recruitment data

Evidence from previous studies assessing the NPA stock have indicated that fishery catches depend almost exclusively on the appearance of new recruits in each year (Somerton & Kikkawa, 1992; Wetherall & Yong, 1986). Thus, increases in catches approximately reflect recruitment events (Kiyota et al., 2016). Because of this strong linkage, an index of recruitment for NPA was calculated based on commercial fishery catch records. The annual catches of NPA from 2002 to 2019 in the NPFC-managed Convention Area of the northeast Pacific were obtained from the NPFC website (www.npfc.int/statistics, accessed August 18, 2020). Historically, no catch limits have existed for NPA; however, a 700 ton encouraged catch limit has been in place for NPFC member countries since 2019. The fishery for NPA is carried out with bottom trawls (Japan and Korea) and gillnets (Japan). Prior to 1990, Russian trawlers also fished for NPA in the SE-NHR; however, these catches were not included in the analysis as Russian fishing ceased after 2006. The catches from Japan and Korea NPA fisheries were summed by year across gear types, and a standardized index of recruitment was generated by dividing the annual catch by the geometric mean of the entire time-series of catches. The geometric mean was used due to the highly right-hand skewed characteristic of the time series where catch values varied over many orders of magnitude.

2.3 | Independent data

2.3.1 | Advection model

The dispersal of larval NPA in this study was simulated using Lagrangian particle tracking from OceanParcels (Probably A Really Computationally Efficient Lagrangian Simulator) version 2.2 (Delandmeter & van Sebille, 2019; Lange & van Sebille, 2017). The OceanParcels framework is designed to generate virtual Lagrangian particle trajectories using ocean circulation model outputs as current fields. Global ocean surface velocity field datasets were obtained from the Globcurrent project at marine.copernicus.eu/ for a 18 year period from 2001 to 2018. The Globcurrent multi-observation product MULTIOBS_GLO_PHY_REP_015_004 (Global Monitoring and Forecasting Center, 2020; Rio et al., 2014) provides daily average ocean surface velocity fields at a ¼ degree spatial resolution from a combination of Copernicus Marine Service satellite geostrophic currents and modeling of Ekman currents.

Although the specific distribution of NPA larvae in the water column remains unknown, individuals have been collected for study via surface drift nets in the top several meters of the ocean (Murakami et al., 2016). Current knowledge of NPA accepts that eggs and early-stage larvae are distributed in the ocean's surface region for the first several months (Boehlert & Sasaki, 1988). Two full Globcurrent field datasets were therefore acquired; one at the ocean surface (0 m depth) and another below the surface at 15 m depth. This allowed us to simulate particles at both depths to account for a range of larval vertical distributions at the ocean surface and to compare particle trajectories between depths. Using the Globcurrent velocity fields, OceanParcels base advection kernels were applied to NPA particles and particle positions were calculated using OceanParcels' default integration, the fourth-order Runge Kutta integration (van Sebille et al., 2018). While OceanParcels has the functionality to program for specific particle behavior within the water column, no description of NPA larval behavior currently exists, and we assumed passive transport for eggs and larvae. Particle trajectories were thus directly dependent on the flow dynamics provided by Globcurrent and OceanParcels' base advection scheme.

Two separate simulation runs were executed over the 2001–2018 study period, one using the 0 m depth dataset and one using the 15 m depth dataset. Previous studies have estimated the NPA spawning period to occur from approximately November to March based on histological and otolith analyses, with peak spawning occurring from December to February (Table 1). To center the estimated

TABLE 1 Historical estimates of spawn timing and pelagic duration for North Pacific armorhead in the Emperor Seamounts

Spawning date	Pelagic duration (days)	Source
December–March	365–1095	Uchiyama and Sampaga (1990)
November–March	365–1642.5	Boehlert and Sasaki (1988)
November–March	1460+	Uchida and Tagami (1984)
November–March	729–999	Humphreys (2000)
Winter	912.5+	Humphreys et al. (1993)
December–February	547.5–912.5	Humphreys et al. (1989)
November–March	730–1642.5	Kiyota et al. (2016)
December–February	912.5+	Murakami et al. (2016)
November–February	912.5–1460	Yonezaki et al. (2017)
December–March	547.5–912.5	Somerton and Kikkawa (1992)

spawning peak, simulations were executed over a period of four winter months from November 15 to March 15. A central point at each of the six study seamounts was designated as a release location (Figure 1), from which particles were deployed daily. A drift trajectory of 120 days was generated for each particle to approximate a potential timeline of swimming capability development. The assumption of active swimming development at 120 days old was utilized previously by Yonezaki et al. (2017) based on the determination of NPA larval standard lengths using the von Bertalanffy growth curve (Murakami et al., 2016). Particle trajectories were recorded, and end points were extracted to give measures of straight line distance (SLD), cumulative distance (CD), end longitude, and end latitude for both depth simulation runs.

2.3.2 | Environmental variables

Two environmental variables were examined for their potential relationship with NPA recruitment: SST and net primary productivity (NPP). SSTs describe the thermal conditions which drive primary production and larval development. NPP is the rate of photosynthetic carbon fixation excluding the fixed carbon used for metabolic processes (Behrenfeld & Falkowski, 1997a). Ocean color models, which utilize satellite-derived chlorophyll-a pigments data to estimate NPP, provide a measure of marine phytoplankton biomass that can act as important environmental data in fisheries studies (O'Reilly et al., 1998; Saba et al., 2011). Stomach content analyses on NPA have shown that their diet is often comprised of zooplankton (Kiyota et al., 2016), which feed on phytoplankton (Solanki et al., 2008). Food resource availability is a principal determinant of pelagic larval fish survival and recruitment (Cury & Roy, 1989), thus relating fish distributions and abundances to remotely sensed seasonal chlorophyll-a and SST variations is often a goal of pelagic fish studies (Lanz et al., 2009; Mugo et al., 2010; Shaari & Mustapha, 2018; Zainuddin, 2011). The daily SSTs and MODIS NPP (surface chlorophyll-a in mg C m^{-2} d^{-1}) were estimated based on values nearest to the daily position of each NPA particle. Temperature estimates were available daily at a ¼° spatial resolution from The Optimum Interpolation Sea Surface Temperature (OISST) analysis v2.1 (www.ncdc.noaa.gov/oisst; Huang et al., 2020). MODIS NPP estimates were available on 8 day intervals from 2002 to 2019 at a ¼° resolution from sites.science.oregonstate.edu/ocean.productivity/ (Behrenfeld & Falkowski, 1997b). The combined dataset consisted of a date, daily position, daily geo-located SST, and geo-located NPP measurements every 8 days for each particle representing an NPA larva released from seamounts in the northeast Pacific.

2.3.3 | Climate indices

The PDO index, defined as the leading principal component of SST variability in the North Pacific (Mantua et al., 1997), shifts between positive and negative regimes depending on the strength of the Aleutian low (Rodionov et al., 2007). When the PDO regime shifts to positive values, the northeast Pacific experiences positive SST anomalies, while negative SST anomalies occur in the central and western North Pacific (Newman et al., 2016). The NPGO index is the second principal component of variability in sea surface height anomalies, and is known to play an important role in driving North Pacific conditions including salinity and chlorophyll-a (Di Lorenzo et al., 2008). The AO index is the leading empirical orthogonal function of sea level pressure in the Northern Hemisphere, and acts predominantly on the Arctic region and a mid-latitude zone over both the North Pacific and the North Atlantic (Hamouda et al., 2021; Thompson & Wallace, 2000).

In addition to the PDO, NPGO, and AO, many other climate indices have been related successfully to fish-based indices. A collection of seven commonly used climate indices was selected for comparison with NPA recruitment. Datasets were obtained from the National Oceanic and Atmospheric Administration (NOAA, US) Climate Prediction Center (www.cpc.ncep.noaa.gov/) for the PDO (Mantua et al., 1997; NOAA National Centers for Environmental Information, 2022), the AO (NOAA Climate Prediction Center, 2022a) and the Ocean Nino Index (ONI; NOAA Climate Prediction Center, 2022b). We obtained the multivariate ENSO Index (MEI, NOAA Physical Sciences Laboratory, 2022), the North Pacific Gyre Oscillation (NPGO; Di Lorenzo et al., 2008; o3d.org/npgo/roms.html), the North Pacific Index (NPI; National Center for Atmospheric Research, 2022; Trenberth & Hurrell, 1994; Wallace & Gutzler, 1981), and the Aleutian Low Pressure Index (ALPI, Surry & King, 2015; www.dfo-mpo.gc.ca/science/documents/data-donnees/climatology-climatologie/alpi-eng.txt).

2.4 | Statistical analyses

2.4.1 | Linear regression

All analyses were conducted with R software version 4.1.1 (R Core Team, 2021). Significance was determined at the $p < 0.05$ level. Since the recruitment index data were available from 2002 to 2019, all other acquired datasets were adjusted to this time period for analyses. The advection dataset was obtained beginning at 2001 to account allow comparison with recruitment data at lags. Particle trajectories and end points were plotted for both depth datasets. End-point density rasters were generated using the R raster package (Hijmans & van Etten, 2012) and were projected in a Mercator projection centered on the North Pacific Ocean. The end-point raster's figures allowed visualization of the particle distribution and density across the simulation fields. Each 1 km^2 cell displays the count of particles situated within the cell area after 120 days of advection with OceanParcels. For each end-point density raster, we calculated center of gravity, skewness, and kurtosis, which were compared using linear regression to the NPA recruitment index.

Linear regression models were used to examine the relationship between the recruitment index and the simulation particle trajectory data (SLD, CD, end longitude, and end latitude). Regression analyses using these variables were performed on trajectories originating during the peak spawning season (December–February). Sensitivity

analyses were also completed on spawning occurring outside of this temporal window (November–March). While estimates of NPA's pelagic period duration (Table 1) have previously varied in length to account for the possibility of other more lengthy migration routes, Boehlert and Sasaki (1988) proposed that the pelagic phase occurs over a period of 1.5 to 2.5 years for fish migrating in the northeastern direction. Trajectory data were thus regressed against the recruitment index with 1 and 2 year lags to account for uncertainty in the period of dispersal to the nursery zone. The ratio of SLD to CD for each trajectory was used as an approximation of vorticity, which was regressed with recruitment to explore the existence of a potential relationship between particle meandering and recruitment.

In order to quantify the advection characteristics of simulated particles, we assigned a zone of particle retention around the spawning habitat at the SE-NHR seamounts and a hypothetical nursery zone in the northeast Pacific. A 200 km-wide buffer was generated around the six seamount release locations to function as a spawning ground retention zone. Particles that ended within this zone were characterized as "retained." Coordinates of historical NPA pelagic occurrences in literature from Boehlert and Sasaki (1988), Murakami et al. (2016), Humphreys et al. (1993), and Humphreys (2000) were plotted as spatial points, around which a polygon was loosely fitted to represent potential nursery grounds (Figure 2). Particles that reached this polygon were considered "nursery zone-advected." We applied mask raster layers of the retention zone and nursery zone over each of the end-point density rasters to compute quantities of particles that dispersed into each zone for every year and to run descriptive statistics. The recruitment index was regressed with the percentages of retained particles and of advected particles at 1 and 2 year lags for the 0 and 15 m depth datasets.

Regression models were additionally used to test for significant relationships between the NPA recruitment index and the seven climate indices. Annual climate index values were evaluated, as well as shorter time period subsets to detect significant relationships between seasonal indices and recruitment. Climate indices for which monthly values were available, including the PDO, the NPGO, the AO, and the NPI, were subset into the following seasons; fall (September–November), winter (December–February), spring (March–May), and summer (June–August). The MEI index values represent two overlapping months; thus, each value was isolated as a subset and regressed with recruitment. This same process was conducted with the ONI index, for which values are a 3-month running mean.

2.4.2 | Generalized additive modeling

Non-linear relationships between recruitment and oceanographic variables were explored with generalized additive models (GAMs) using the mgcv package in R (Wood, 2006; Wood, 2011). Recruitment (y) was modeled as a smoothed function of temperature variables and productivity variables:

$$y = s_{\text{temperature}} + s_{\text{productivity}} + \varepsilon,$$

where s indicates a thin-plate regression spline and the errors, ε, are normally distributed. Recruitment was log-transformed to meet the assumption of normality. Two temperature variables were obtained for use as GAM predictor variables; the annual mean SST calculated along the particle trajectory path, and the annual mean number of degree-days calculated using a base temperature of 9°C (Chezik et al., 2014). Two productivity variables, the annual mean NPP along the path of simulated larval drift and the cumulative NPP since January 1 along-path of the larval drift, were similarly obtained as predictor variables. Variable selection was conducted to reduce unnecessary model complexity using a combination of approximate p value, estimated degrees of freedom and generalized cross-validation score (GCV; Wood, 2006). Mean SST and mean degree days were highly correlated and generated identical GAMs with each productivity variable. Since this too was the case for the productivity variables, only one of each variable type was necessary for subsequent GAM analyses, and mean SST and mean NPP were set as GAM covariates.

Relative model fits to the data were evaluated using the Akaike information criterion corrected for small sample sizes (Burnham & Anderson, 2002). To reduce overfitting on such a small dataset, a basis degrees of freedom of $k = 4$ was used in each GAM to decrease the number of potential inflection points in the smoothed fit. Although GAMs are fairly robust to violations of assumptions of normality, the model residuals were examined to detect for any violations of this assumption. To determine the best model fit to data, exploratory model analyses also evaluated alternative error structures for all GAMs, including the Tweedie and gamma distributions. Neither of these distributions resulted in improved model diagnostics over the Gaussian distribution.

3 | RESULTS

3.1 | Recruitment index

The catches of NPA in the SE-NHR region ranged from 242 metric tons (mt) in 2016 to 25,460 mt in 2012 (mean = 5221 mt, sd = 7674 mt). The index of recruitment computed from the geometric mean of the catch time series ranged from approximately 0 to 12.9 over the 18 years of data (Figure 3). Most years experienced low recruitment, with peaks occurring in 2004, 2008, 2010, and 2012.

3.2 | Advection model

Over the simulation, a total of 20,568 particles were released (10,284 at each depth). Mean SLD travelled by particles after 120 days was approximately 860 km for the 0 m depth dataset particles, and 710 km at 15 m depth. Mean CD was approximately 2,220 km at 0 m depth and 2,050 km at 15 m depth. Mean end particle latitude was 32.6°N for both the 0 depth dataset and for the 15 m depth dataset, while mean end longitudes were 162.3°W longitude

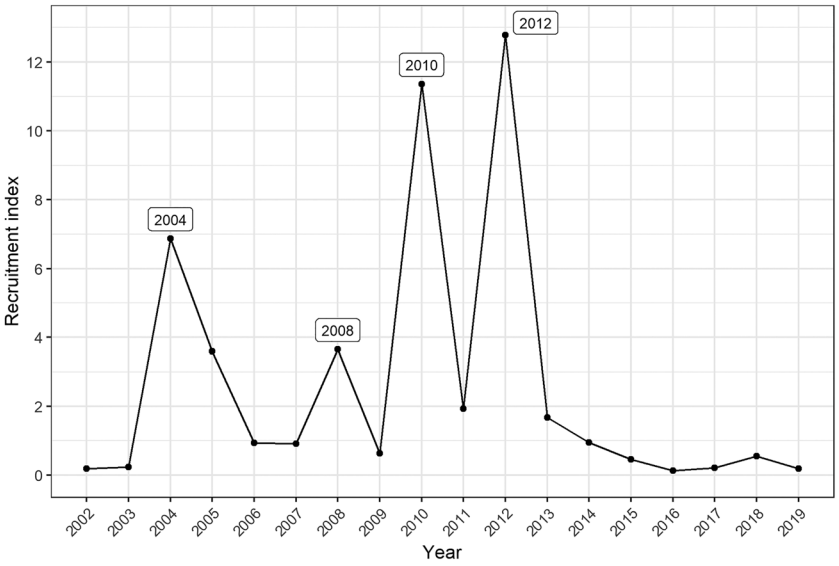

FIGURE 3 NPA recruitment time series calculated from the annual catch by Japan and Korea. Labeled years indicate recruitment peaks.

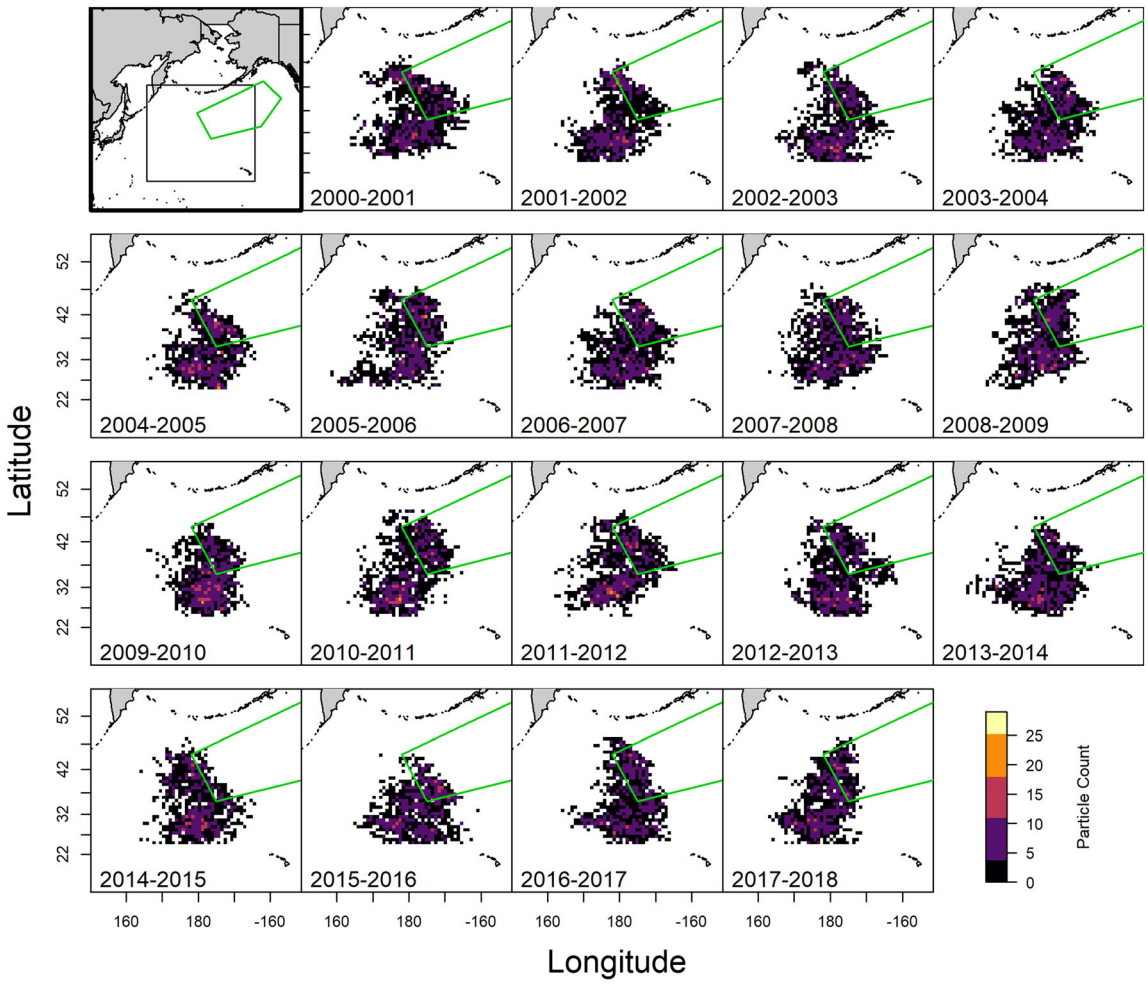

FIGURE 4 Raster plots showing the nursery zone (green polygon), and the density and distribution of particles in the northeast Pacific ocean after 120 days of advection with OceanParcels at 0 m depth. Each cell that displays a particle count outlined by the legend covers an area of 1 km^2. The top left grid panel displays the full North Pacific study area and includes a smaller rectangle, which depicts the bounds of the other panels in the plot.

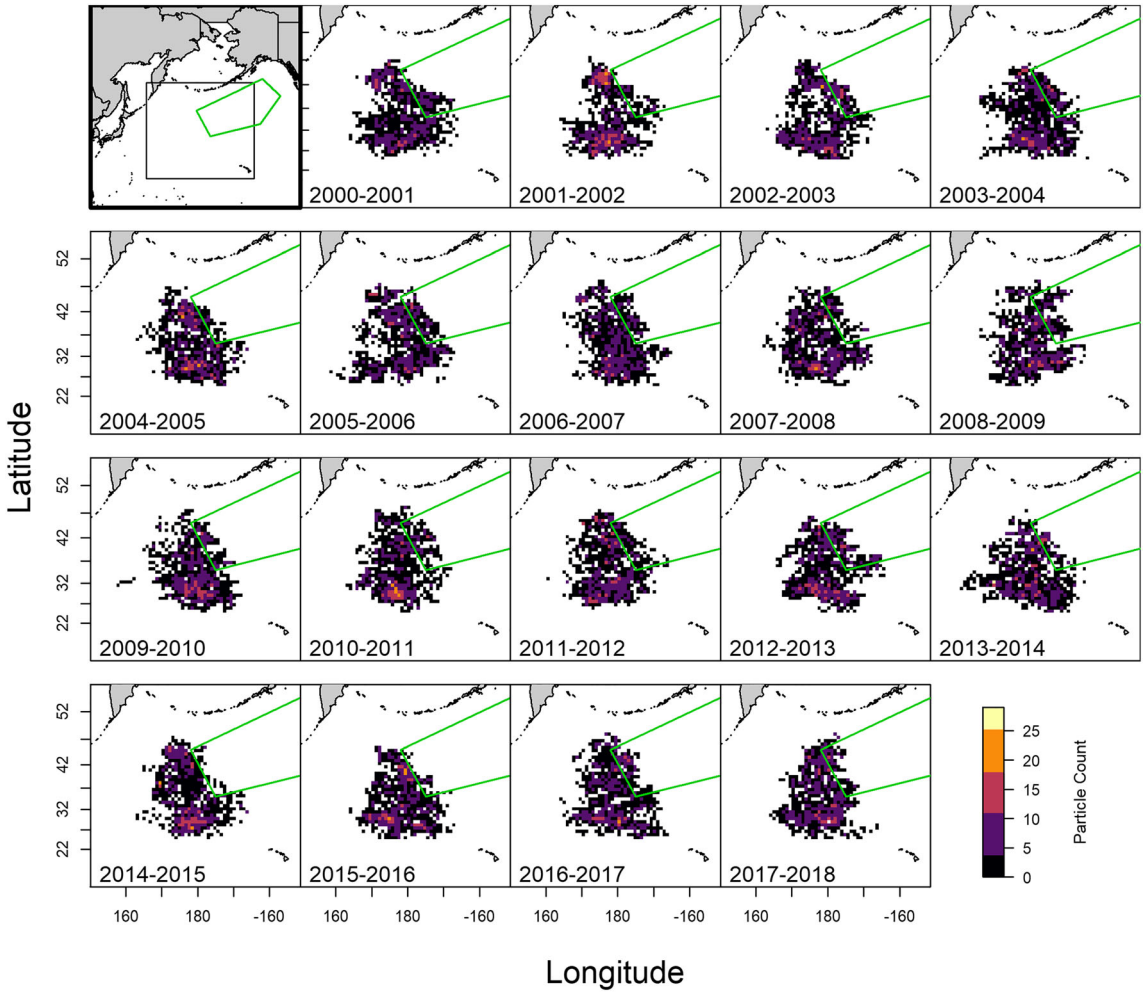

FIGURE 5 Raster plots showing the nursery zone (green polygon), and the density and distribution of particles in the northeast Pacific ocean after 120 days of advection with OceanParcels at 15 m depth. Each cell that displays a particle count outlined by the legend covers an area of 1 km^2. The top left grid panel displays the full North Pacific study area and includes a smaller rectangle, which depicts the bounds of the other panels in the plot.

and 164.6°W longitude at 0 and 15 m depths, respectively. Regression of the 0 and 15 m depth datasets revealed no significant relationships between recruitment and SLD, CD, end longitude, or end latitude. A marginally insignificant negative linear relationship ($p = 0.06$, $R^2 = 0.155$) occurred between recruitment and CD at depth 15 m at a lag of 2 years. Sensitivity analyses assessed the inclusion of spawning months November and March but did not produce meaningfully different results to when the analysis was constrained to the peak spawning period from December to February. Vorticity, calculated as the ratio of SLD to CD, was not a significant predictor of recruitment at either depth.

The drift trajectories in most years indicated that many particles at both 0 m (Figure 4) and 15 m (Figure 5) drifted to the northeast from the seamounts, and that particles simulated at 0 m depth tended to exhibit a wider dispersal. The end-point rasters displayed areas of peak concentration in all years. In many years (e.g., panel 2001–2002 in Figure 4), a bimodal pattern of end points was apparent, where one high density patch of larvae occurred to the northeast, and one to the southeast closer to the SE-NHR. All end-point rasters for both depths had positive skewness values consistent with non-uniform and non-normal dispersal. Kurtosis values indicated relatively flat distribution of points throughout the rasters for both depths. No clear relationship was found when recruitment was tested against the measures of center of gravity, skewness and kurtosis for the 0 m and 15 m depth rasters. On average, a larger quantity of 0 m depth-simulated particles reached the nursery zone compared to the 15 m depth dataset. Percentages of nursery-zone advected particles were not found to be extraordinarily high; values over the simulation period fell between 9.1%–36.8% for the 0 m depth dataset (Figure 6), and 2.6%–17.8% for the 15 m depth dataset (Figure 6). Particles were also not retained at the SE-NHR in high percentages; between 1.8–10.3% of particles were retained at 0 m depth and 2.7–12.4% were retained at 15 m depth (Figure 6). Figure 7 shows the cumulative particle distributions across all simulation years for each depth in relation to the SE-NHR seamounts and the nursery zone. No linear relationships were found between recruitment lagged at 1 or 2 years and percentages of retained or advected particles at 0 or 15 m depth.

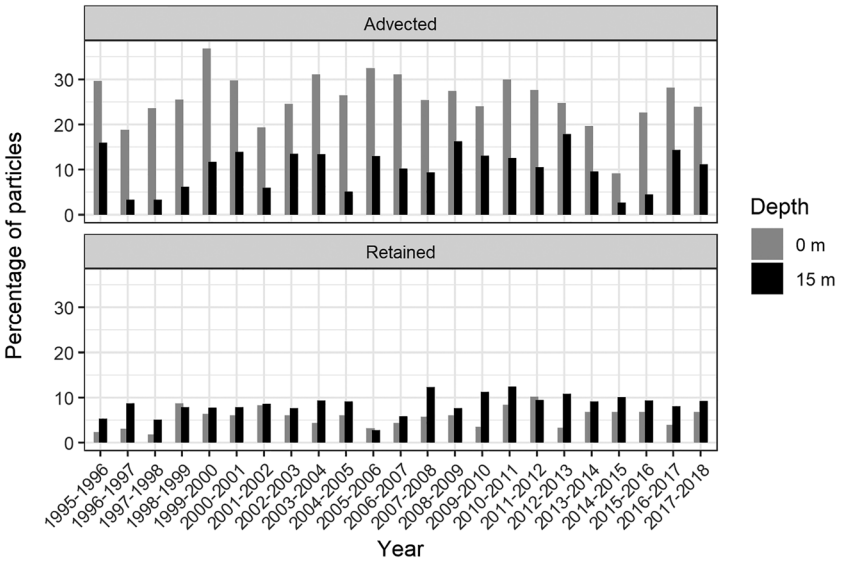

FIGURE 6 Percentages of simulated particles advected to the proposed northeast Pacific nursery zone and percentages of particles retained adjacent to the SE-NHR spawning grounds are shown for the 0 and 15 m depth datasets.

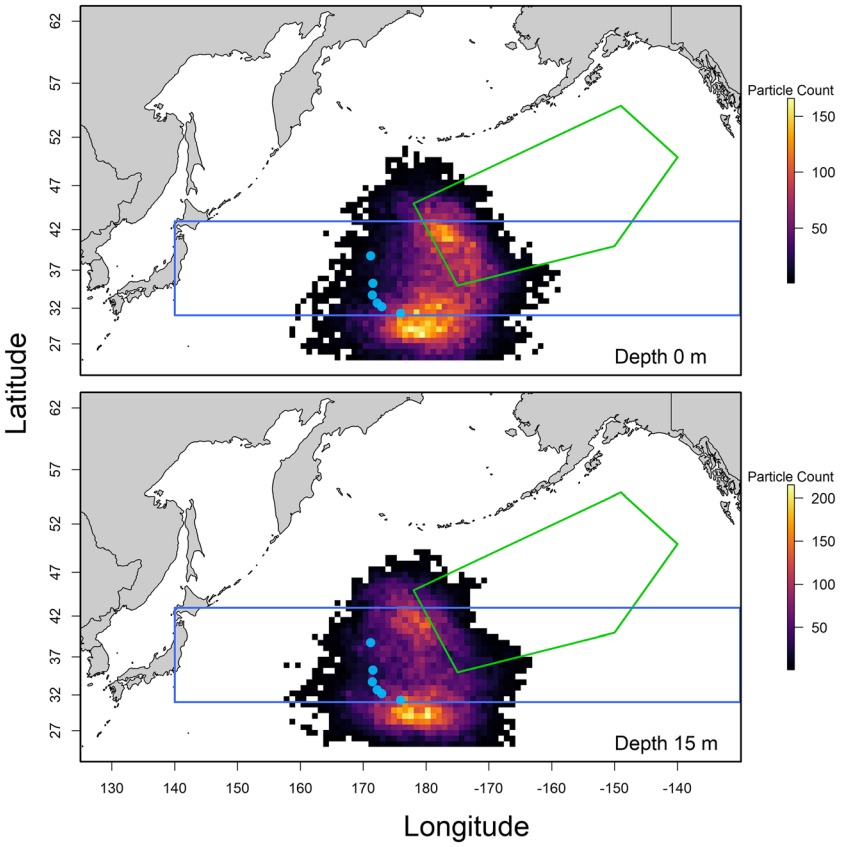

FIGURE 7 Raster plots showing the total particle count in each 1 km^2 cell summed across all years from Figures 4 and 5 for each depth. The green polygon represents this study's nursery zone, and the blue polygon represents an approximate location of the North Pacific Transition Zone. The blue circular points indicate the locations of the six study seamounts.

3.3 | Environmental variables

The SSTs encountered by our simulated particles at the ocean surface ranged from 13.42°C to 24.81°C, with a mean of 17.2°C (1.44°C standard deviation [sd]). The mean NPP was 577.21 mg C m^{-2} day^{-1} (205.44 mg C m^{-2} day^{-1} sd), with a range of 239.27 to 5233.3 mg C m^{-2} day^{-1}. The GAMs did not show significant correlations with the predictor variables as judged by the approximate p-values. However, the GAM that used mean SST and mean NPP to predict log recruitment explained 23.1% of the deviance in the data (Figure 8). The GAM partial effect plots showed that recruitment decreased linearly with increasing SST ($p = 0.09$). The effect of NPP as a predictor variable was highly insignificant ($p = 0.76$), though the partial effects plot appears to illustrate a potential optimal relationship with the index of recruitment at intermediate productivity values (NPP $\sim$ 600 mg C m^{-2} day^{-1}).

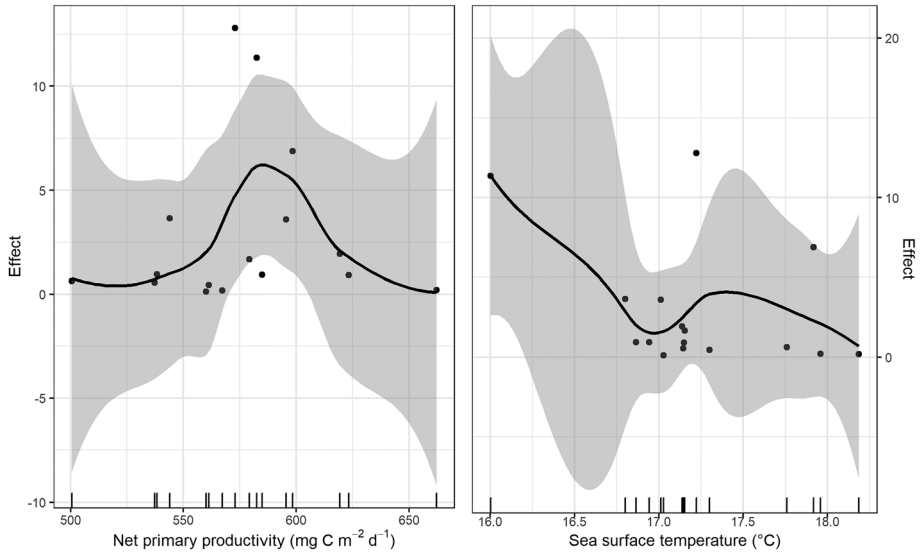

FIGURE 8 Partial plots of estimated smoothness of SST and NPP for the best-fitting generalized additive model. The partial effect of the variable is shown on the *y* axis, and the shadow section represents one standard deviation.

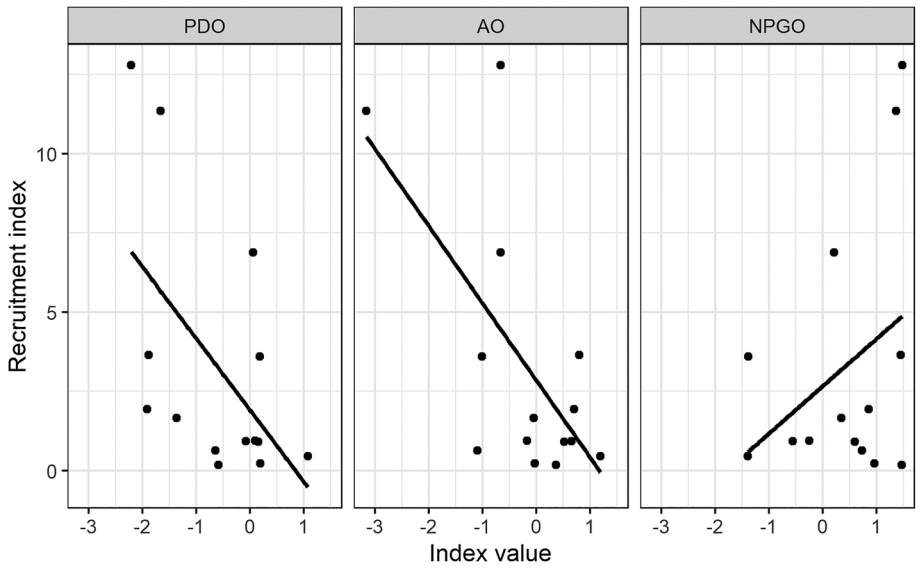

FIGURE 9 Shown are regression plots of NPA recruitment and climate indices where a significant linear relationship was found. Climate data shown are seasonal; index values for the PDO are from summer months (June–August), values for the AO are from winter months (December–February), and values for the NPGO are from spring months (March–May).

3.4 | Climate indices

Three of the seven climate indices had significant linear relationships with the NPA recruitment index. The index of recruitment was found to correlate with the PDO during summer months from June to August ($p = 0.01$), with the model explaining approximately 35% of the variability in recruitment ($R^2 = 0.35$; Figure 9). A significant negative regression was found between recruitment and AO values during winter months from December to February ($R^2 = 0.435$, $p = 0.003$; Figure 9). During spring months from March to May, the NPGO was found to have a moderately significant positive relationship with recruitment ($R^2 = 0.23$, $p = 0.04$; Figure 9). Significant relationships were not found between the index of recruitment and climate indices including the ALPI ($p = 0.10$), the MEI ($p = 0.09$), the NPI ($p = 0.51$), and the ONI (0.26) using linear regression.

4 | DISCUSSION

We employed Lagrangian particle analysis to investigate potential correlations between physical transport in the North Pacific ocean and recruitment in NPA. Trajectory simulations resulted in areas of high concentrations of particle end points, and notable percentages of particles that were advected to the northeast of the SE-NHR. The recruitment index was not found to be significantly related to trajectory variables for particles released during the spawning season,

however significant correlations resulted from regression of prominent North Pacific ocean-climate indices against the index of NPA recruitment. Based on the GAM analysis results, we suggest that an important association between recruitment and SST may exist.

4.1 | Recruitment analysis

Given the pronounced differences in NPA abundance year-to-year, stock-independent factors such as environmental processes have been proposed to drive a large portion of the annual NPA recruitment variation (Wetherall & Yong, 1986). The recruitment index for this analysis was calculated from the geometric mean of the catch, which assumes that NPA recruitment events are solely the cause of biomass fluctuations and commercial catch is a direct representation of recruitment. While this assumption has been made in previous NPA studies (Somerton & Kikkawa, 1992), it may be problematic to rely on catch data to calculate a recruitment index considering the uncertainties in year-class strength drivers for the species.

As catch data were only available for 18 years, our study period was constrained to a relatively short time series. The presence of high and low recruitment events provided contrast for exploration in this study; however, analyses of long-term environmental variability and dispersal patterns were not possible with existing data availability.

4.2 | Behavior and habitat

Six central SE-NHR seamounts surrounding the historical center of NPA abundance were chosen as particle release locations. For species that have strong associations with a specific habitat, such as demersal NPA with seamount habitat post-settlement, habitat can be used as a reliable proxy for spawning location (Swearer et al., 2019). Among the central seamounts, however, there are notable differences in topography, productivity, assemblages, and fishing histories (Sasaki, 1986). Yonezaki et al. (2017) found that quantities of advected particles arriving from different origin seamounts to the nursery area after 120 days were substantially different, with particles originating from Jingu almost three times more prevalent than Koko, and Kammu-originated particles making up only 0.1%. Because spawning at specific locations is an important determining factor of end-point locations and success for many fish species (Schilling et al., 2020) and NPA dispersal trajectories may differ considerably between seamounts, current data on NPA spawning events would be valuable to the study of this species.

As the exact timing and location of NPA batch spawning events remain unknown, particles were deployed at a constant daily rate over the study simulation period to account for variability in oceanographic conditions, producing maps of potential end points from each day of the spawning season. Consequently, it is likely that true NPA larvae locations after 120 days in the ocean differ somewhat from our simulated particle end points. Patches of high densities of larvae end points similar to those shown in Figures 4 and 5 were expected to occur due to current patterns and mesoscale eddies, which can entrain larvae and produce areas of comparatively higher concentrations (Lobel & Robinson, 1986). It is possible that in nature, these concentrated patches may occur at even higher densities than those generated in this study using a uniform temporal particle dispersal. While factors relating to current transport alone could be responsible for the presence of high-density particles areas, particle clustering could also point towards evidence for early schooling behavior, which has been suggested for NPA but not well-documented (Boehlert & Sasaki, 1988).

A point of significant uncertainty in this study and others is the absence of data on the development of NPA movement behaviors throughout the epipelagic phase. There is evidence that fish in early developmental stages may be able to exhibit vertical movement in the water column in response to light, food and predation, as well as to detect and avoid turbulence (Olla & Davis, 1990; Swearer et al., 2019). While it seems plausible that in later larval stages NPA would begin to exhibit more complex behavior, such as horizontal swimming, programming of complex particle behavior during our simulations was not possible due to the lack of data. Significant differences in larval transport can be produced by small vertical positional changes and horizontal movements within the water column; thus, knowledge of depth distribution and behavior is important in dispersal modelling (Swearer et al., 2019). Further data on the developmental timeline of NPA larvae would be required to include larval movement into biophysical modeling; however, there are no current viable means to acquire this data. Assessment of pelagic NPA would involve long, expensive surveys and likely low encounter probability given the vastness of the potential grounds in which they may be found.

4.3 | Advection and nursery zone

Our results show that many of the simulated particles were located somewhere between the SE-NHR and the designated nursery zone at the end of 120 days (Figure 7); particle retention at the SE-NHR was not strong at either depth and neither dataset produced exceedingly high percentages of nursery zone-advected particles. Murakami et al. (2016) proposed that larval NPA that occur near 32°N could likely be entrained in an east-northeast geostrophic current, sending them in the direction of the hypothesized nursery zone. As our six release seamounts are located from approximately 31.3°N to 38.8°N, this current may contribute to our particle end point distributions. Particles advected at 0 m depth had greater mean SLDs and CDs and reached more eastern longitudes compared to the 15 m depth particles, which is logical due to faster-moving currents at the ocean surface. At both 0 and 15 m depths, recorded mean SLDs were much shorter than mean CDs indicating a meandering of particles during their trajectory, though a direct correlation between our measure of vorticity and recruitment was not found. The trajectory variables we investigated did not present strong relationships with the recruitment index. Narrowing the particle deployment period from November–March to December–February to simulate the peak spawning season raised

significance of the relationship, albeit only marginally. The lack of strong relationships here between recruitment and advection variables may suggest that a small amount of variability in larval positions within the northeast Pacific may not have a significant impact on recruitment, or at least not at 120 days.

This study's nursery zone polygon was based on historical occurrence data points from Boehlert and Sasaki (1988), Murakami et al. (2016), and Humphreys et al. (1993, 2000). The polygon, similar to that depicted in Murakami et al. (2016), covered an area of ocean in the northeast Pacific from 178°E to 140°W, and 35°N to 55°N (Figure 2). Our analysis was not able to model a correlation between dispersal to a particular nursery zone and recruitment. However, some combination of advection and active movement after the first 120 days could propel NPA within a similar area to the nursery zone tested in this work. A distinct spatial separation between year classes across the eastern North Pacific has been described previously, where younger specimens are found closer to the SE-NHR region and larger specimens occur northward and eastward (Boehlert & Sasaki, 1988; Murakami et al., 2016). Following this pattern, perhaps larvae at 120 days are merely still in transit toward optimal nursery conditions. Alternatively, perhaps what can be characterized as NPA nursery grounds is very broad, either encompassing a large spatial area or several areas with ideal conditions for various life stages.

4.4 | Environmental variables

SST, a widely used environmental indicator and GAM variable in fisheries studies, has been found to be the best predictor for habitat (Lien et al., 2014; Mugo et al., 2010) and abundance from CPUE (Abdellaoui et al., 2017) for other pelagic species. The GAM methods employed in this analysis showed a potential negative relationship between water temperature and NPA recruitment, although the relationship was not statistically significant. Since temperature affects fish larvae both directly by acting on their larval development rate, and indirectly through effects on production of prey (Otterson & Loeng, 2000), it is likely correlations between NPA and SST patterns or surface thermal features do exist despite not being illustrated here using this index of recruitment.

Epipelagic NPA have been collected in temperatures between 8.6°C and 15°C (Boehlert & Sasaki, 1988) and have been found to occur within significantly different mean SSTs based on their age class during summer sampling in the nursery zone (Murakami et al., 2016). The SSTs encountered by our simulated particles ranged from 13.42°C to 24.81°C, the lower end of which is comparable to the approximate temperatures where age 0 class fish were found to occur by the Murakami et al. (2016) study. In Murakami et al. (2016), NPA appeared to prefer lower SSTs with increasing age. Within the range of temperatures found in this study, relatively low SSTs were associated with more northern latitudes encountered by particles. Northeastward-directed advection after 120 days would presumably follow this pattern, with older fish occurring in increasingly lower SSTs as noted by Murakami et al. (2016).

NPP, or ocean color data, is often assessed alongside SSTs as an environmental driver of fish abundance and distribution, as SSTs and chlorophyll-a are often tightly linked (Behrenfeld, 2014; Behrenfeld et al., 2006; Solanki et al., 2005) and their covariance is highly dependent on regional conditions (Dunstan et al., 2018). The ocean color variable used in our GAMs was not found to be a significant predictor for NPA recruitment. These results could indicate a weak relationship between the two or could likely be attributed to the indices used in this work to compare the primary production level to NPA larvae several trophic levels above. Although insignificant, there did appear to be a possible optimal relationship between the index of recruitment and NPP, shown in Figure 8. Given the trophic separation between NPA and phytoplankton, it is difficult to decipher the true relationship between them. In some marine food webs, abundances of phytoplankton, zooplankton, and pelagic fish do not necessarily overlap spatially and temporally, producing a mismatch between trophic levels (Grémillet et al., 2008).

Zooplankton, which have been found by past studies to be central prey items to NPA diets (Kiyota et al., 2016; Nishida et al., 2016), are known to aggregate at the Transition Zone Chlorophyll Front (Glover et al., 1994; Polovina et al., 2001). The front migrates seasonally within the North Pacific transition zone from approximately 31°N to 43°N (Polovina et al., 2017), and is known to be an important foraging environment for various epipelagic species including Pacific saury, Pacific pomfret and mackerel species due to the enhanced trophic exchange (Pearcy, 1991). When plotted spatially, a large number of our particle end points for both years appear to fall within the transition zone (Figure 7). In fact, the bimodal particle density spatial pattern that appears at both depths in many years (Figures 4 and 5) and cumulatively in Figure 7 generally aligns with the transition zone northern boundary at the Subarctic Front and the southern boundary with the Subtropical Front. These boundaries are characterized by localized regions of higher productivity. Given the occurrence of NPA within the transition zone boundaries as spawning adults and likely during some periods of their epipelagic phase, favorable NPA foraging conditions are expected to be produced during at least some of the year within the transition zone.

4.5 | Climate

Three climate indices were found to be significantly related to the index of recruitment; the AO, the NPGO, and the PDO. Wintertime AO values ($p = 0.003$) and PDO during summer months ($p = 0.01$) were negatively correlated to recruitment. A similar relationship with PDO was observed previously by Yonezaki et al. (2017), where catch of NPA was relatively low during positive PDO phases. PDO phase changes have been shown to correspond to water mass transports and related temperature-dependent zooplankton community changes in the North Pacific (Di Lorenzo et al., 2013; Hipfner et al., 2020) and have caused dramatic and opposite effects in fish stocks historically (Peterson & Schwing, 2003). Pacific Salmon are a well-studied example of this; PDO-related climate forcing drives changes in zooplankton

abundance and species composition, which are tracked by regional trends in salmon (Graham et al., 2021; Keister et al., 2010). How NPA catch and recruitment relate mechanistically to the PDO was not distinguished by Yonezaki et al. (2017) and remains unclear in the present study. It is possible, however, that a bottom-up correlation between zooplankton and the PDO could translate into the PDO-NPA relationship found here.

A moderate correlation was found between recruitment and the NPGO during spring months between March to May. Murakami et al. (2016) previously suggested a link between NPA larval transport and phases of the NPGO, which is characterized as the second leading principal component of northeast Pacific sea surface height anomalies (Di Lorenzo et al., 2008). A strong geostrophic current between the SE-NHR region and the nursery zone to the northeast is proposed to strengthen during positive NPGO index phases, which could transport larvae directly towards the posited nursery zone (Murakami et al., 2016). If this effect is captured by the NPGO, it is reasonable that the relationship would be strongest in spring, when larvae are passive and located at the ocean's surface following the spawning season.

The dominant climate modes of the northeast Pacific, such as the PDO and the NPGO, reflect different sources of wind and circulation variability (Coffin & Mueter, 2016), and relationships between indices fluctuate through time (Litzow et al., 2020). As stated by Newman et al. (2016) regarding the PDO, climate indices reflect patterns that are forced by a combination of many physical processes occurring at varying time scales. The complexities driven by climate oscillations render discerning the true impact of each mechanism on NPA, their prey, and their surrounding physical conditions extremely difficult. Presumably, climate-ocean forcing captured by indices including the AO, PDO and NPGO exerts a host of direct and indirect influences on NPA beyond what was captured by the data and modeling within this study.

5 | CONCLUSIONS

The results of this study showed that there are clear linkages between basin-scale oceanographic conditions and NPA recruitment. While statistical correlations were not found here between larval advection to the nursery polygon and recruitment success for this time series, a significant proportion of simulated particles were located between the spawning grounds and the supposed nursery grounds after 120 days of advection with OceanParcels. The distributions of particle end points were found to coincide with the North Pacific transition zone. This may point to broadly-defined nursery grounds for NPA, or may suggest that juveniles are largely being advected through the transition zone during early stages of the pelagic phase, followed by a farther-reaching active migration later in the pelagic phase.

An extended time series of NPA recruitment may allow for better comparison with climate modes or temperature and productivity regimes. Advection predictions could be greatly improved with a better understanding of NPA behavioral ecology, particularly of the specific timeline of horizontal swimming development. More comprehensive data on broad conditions of the northeast Pacific nursery zone and the species-specific relationship with SST and seasonal prey conditions would aid in deciphering the ideal conditions for early development of NPA and how their pelagic migrations are advantageous for their life history.

The fishery for NPA at the Emperor Seamounts since 2019 has been managed only through effort controls on vessels from Japan participating in the fishery, with encouraged catch limits depending on the estimated level of recruitment (NPFC, 2021). As such, the fishery currently relies on the periodic appearance of strong year classes that are heavily fished, removing most of the newly settled recruits (Kiyota et al., 2013; Somerton & Kikkawa, 1992). The fishery catches then remain depressed until the next large year class appears. Knowledge of the linkages between recruitment and the environment will allow for more informed management of the stock by the North Pacific Fisheries Commission.

ACKNOWLEDGMENTS

The authors would like to thank Dr. Alex Zavolokin and the North Pacific Fisheries Commission scientists, who commented and assisted with guiding this analysis. This work originated from a University of Victoria undergraduate cooperative research project conducted by M. Lavery.

CONFLICT OF INTEREST

The authors confirm that this is an original manuscript, the contents of which have not been published elsewhere and which are not currently under consideration for publication elsewhere. The authors have no conflicts of interest to disclose.

AUTHOR CONTRIBUTIONS

The study design was conceptualized by CR and MAKL, assisted by KF and approved by all contributors. Data acquisition, statistical modeling, and interpretation of results were performed by MAKL and CR. The manuscript was drafted by MAKL and CR and edited by KF and KS. All authors contributed to the review and approval of the manuscript.

DATA AVAILABILITY STATEMENT

All data used to support the findings of this study are openly available in public domains. These data were derived from the following resources: NPFC Science (www.npfc.int/statistics), NOAA National Centers for Environmental Information (Huang et al., 2020; www.ncei.noaa.gov/products/optimum-interpolation-sst and www.ncdc.noaa.gov/teleconnections/pdo/), NOAA Climate Prediction Center (origin.cpc.ncep.noaa.gov/products/analysis_monitoring/ensostuff/ONI_v5.php and origin.cpc.ncep.noaa.gov/products/precip/CWlink/daily_ao_index/ao.shtml), NOAA Physical Sciences Laboratory (psl.noaa.gov/enso/mei/), Di Lorenzo et al., 2008 (o3d.org/npgo/roms.html), Surry & King, 2015 (www.dfo-mpo.gc.ca/science/documents/data-donnees/climatology-climatologie/alpi-eng.txt), National Center for Atmospheric Research (climatedataguide.ucar.edu/climate-data/north-pacific-np-index-trenberth-and-hurrell-monthly-and-winter), and the Oregon State University Ocean Productivity database (sites.

science.oregonstate.edu/ocean.productivity/index.php). This study was conducted using E.U. Copernicus Marine Service Information; Globcurrent multi-observation product MULTIOBS_GLO_PHY_REP_015_004 (10.48670/moi-00050; Rio et al., 2014). Code developed to process OceanParcels netCDF output files for mapping and data extraction is available in our NPA Larval Drift package (github.com/rooperc4/NPALarvalDrift).

ORCID

Madeline A. K. Lavery https://orcid.org/0000-0003-2709-6279
Vladimir Kulik https://orcid.org/0000-0003-0920-5312

REFERENCES

Abdellaoui, B., Berraho, A., Falcini, F., Santoleri, J. R., Sammartino, M., Pisano, A., Idrissi, M. H., & Hilim, K. (2017). Assessing the impact of temperature and chlorophyll variations on the fluctuations of sardine abundance in AL-Hoceima (South Alboran Sea). *Journal of Marine Science: Research and Development*, *7*(4), 1–11. https://doi.org/10.4172/2155-9910.1000239

Beamish, R. J., & Bouillon, D. R. (1993). Pacific salmon production trends in relation to climate. *Canadian Journal of Fisheries and Aquatic Sciences*, *50*, 1002–1016. https://doi.org/10.1139/f93-116

Behrenfeld, M. J. (2014). Climate-mediated dance of the phytoplankton. *Nature Climate Change*, *4*, 880–887. https://doi.org/10.1038/nclimate2349

Behrenfeld, M. J., & Falkowski, P. G. (1997a). A consumer's guide to phytoplankton primary productivity models. *Limnology and Oceanography*, *42*(7), 1479–1491. https://doi.org/10.4319/lo.1997.42.7.1479

Behrenfeld, M. J., O'Malley, R. T., Siegel, D. A., McClain, C. R., Sarmiento, J. L., Fieldman, G. C., Milligan, A. J., Falkowski, P. G., Letelier, R. M., & Boss, E. S. (2006). Climate-driven trends in contemporary ocean productivity. *Nature*, *444*, 752–755. https://doi.org/10.1038/nature05317

Behrenfeld, M. J., & Falkowski, P. G. (1997b). Photosynthetic rates derived from satellite-based chlorophyll concentration. *Limnology and Oceanography*, *42*(1), 1–20. https://doi.org/10.4319/LO.1997.42.1.0001

Boehlert, G. W., & Sasaki, T. (1988). Pelagic biogeography of the armorhead *Pseudopentaceros wheeleri*, and recruitment to isolated seamounts in the North Pacific Ocean. *Fish. Bull. US*, *86*, 453–465. PMID: https://swfsc-publications.fisheries.noaa.gov/publications/CR/1988/8816.PDF

Boehlert, G. W., Wilson, C. D., & Mizuno, K. (1994). Populations of the Sternoptychid fish *Maruolicus muelleri* on seamounts in the central North Pacific. *Pacific Science*, *48*(1), 57–69.

Burnham, K. P., & Anderson, D. R. (2002). *Model selection and multimodel inference: A practical information-theoretic approach*. Springer.

Chavez, F. P., Ryan, J., Lluch-Cota, S. E., & Ñiquen, C. M. (2003). From anchovies to sardines and back: Multidecadal change in the Pacific Ocean. *Science*, *299*(5604), 217–221. https://doi.org/10.1126/science.1075880

Chezik, K. A., Lester, N. P., & Venturelli, P. A. (2014). Fish growth and degree-days I: Selecting a base temperature for a within-population study. *Canadian Journal of Fisheries and Aquatic Sciences*, *71*(1), 47–55. https://doi.org/10.1139/cjfas-2013-0295

Chhak, K. C., di Lorenzo, E., Schneider, N., & Cummins, P. F. (2009). Forcing of low-frequency variability in the Northeast Pacific. *Journal of Climate*, *22*(5), 1255–1276. https://doi.org/10.1175/2008JCLI2639.1

Chikuni, S. (1970). On gregarious fish, *Pseudopentaceros richardsoni* (Histiophoridae). Enyo (Far Seas) Fish. Res. Lab. News 3, 1-4. (Engl. transl., The "phantom fish," "kusakaritubodai" - an outline, English translation by J.H. Shohara, 7 p.).

Coffin, B., & Mueter, F. (2016). Environmental covariates of sablefish (*Anplopoma fimbria*) and Pacific Ocean perch (*Sebastes alutus*) recruitment in the Gulf of Alaska. *Deep Sea Research Part II: Topical Studies in Oceanography*, *134*, 194–209. https://doi.org/10.1016/J.DSR2.2015.02.016

Cury, P., & Roy, C. (1989). Optimal environmental window and pelagic fish recruitment success in upwelling areas. *Canadian Journal of Fisheries and Aquatic Sciences*, *46*, 670–680. https://doi.org/10.1139/f89-086

Delandmeter, P., & van Sebille, E. (2019). The parcels v2.0 Lagrangian framework: New field interpolation schemes. *Geoscientific Model Development*, *12*(8), 3571–3584. https://doi.org/10.5194/gmd-12-3571-2019

Di Lorenzo, E., Combes, V., Keister, J. E., Strub, P. T., Thomas, A. C., Franks, P. J. S., Ohman, M. D., Furtado, J. C., Bracco, A., Bograd, S. J., Peterson, W. T., Schwing, F. B., Chiba, S., Taguchi, B., Hormazabal, S., & Parada, C. (2013). Synthesis of Pacific Ocean climate and ecosystem dynamics. *Oceanography*, *26*(4), 68–81. https://doi.org/10.5670/oceanog.2013.76

Di Lorenzo, E., Schneider, N., Cobb, K. M., Franks, P. J. S., Chhak, K., Miller, A. J., McWilliams, J. C., Bograd, S. J., Arango, H., Curchitser, E., Powell, T. M., & Rivière, P. (2008). North Pacific Gyre Oscillation links ocean climate and ecosystem change. *Geophysical Research Letters*, *35*, L08607. https://doi.org/10.1029/2007GL032838

Dunstan, P. K., Foster, S. D., King, E., Risbey, J., O'Kane, T. J., Monselesan, D., Hobday, A. J., Hartog, J. R., & Thompson, P. A. (2018). Global patterns of change and variation in sea surface temperature and chlorophyll a. *Scientific Reports*, *8*(1), 1–9. https://doi.org/10.1038/s41598-018-33057-y

Global Monitoring and Forecasting Center. (2020). MULTIOBS_GLO_PHY_REP_015_004, E.U. Copernicus Marine Service Information. https://doi.org/10.48670/moi-00050

Glover, D. M., Wroblewski, J. S., & McClain, C. R. (1994). Dynamics of the transition zone in coastal zone color scanner-sensed ocean color in the North Pacific during oceanographic spring. *Journal of Geophysical Research*, *99*, 7501–7511. https://doi.org/10.1029/93JC02144

Graham, C., Pakhomov, E. A., & Hunt, B. P. V. (2021). Meta-analysis of salmon trophic ecology reveals spatial and interspecies dynamics across the North Pacific Ocean. *Frontiers in Marine Science*, *8*, 1–17. https://doi.org/10.3389/fmars.20

Grémillet, D., Lewis, S., Drapeau, L., van der Lingen, C. D., Huggett, J. A., Coetzee, J. C., Verheye, H. M., Daunt, F., Wanless, S., & Ryan, P. G. (2008). Spatial match-mismatch in the Benguela upwelling zone: Should we expect chlorophyll and sea-surface temperature to predict marine predator distributions? *Journal of Applied Ecology*, *45*(2), 610–621. https://doi.org/10.1111/j.1365-2664.2007.01447.x

Hamouda, M. E., Pasquero, C., & Tziperman, E. (2021). Decoupling of the Arctic oscillation and North Atlantic Oscillation in a warmer climate. *Nature Climate Change*, *11*, 137–142. PMID: https://www.nature.com/articles/s41558-020-00966-8

Hijmans, R. J., & van Etten, J. (2012). Raster: Geographic analysis and modeling with raster data. R package version 3.4-5. https://CRAN.R-project.org/package=raster

Hipfner, J. M., Galbraith, M., Bertram, D. F., & Green, D. J. (2020). Basin-scale oceanographic processes, zooplankton community structure, and diet and reproduction of a sentinel North Pacific seabird over a 22-year period. *Progress in Oceanography*, *182*, 102290. https://doi.org/10.1016/j.pocean.2020.102290

Houde, E. D. (2008). Emerging from Hjort's shadow. *Journal of Northwest Atlantic Fishery Science*, *41*, 53–70. https://doi.org/10.2960/J.v41.m634

Huang, B., Liu, C., Banzon, V., Freeman, E., Graham, G., Hankins, B., Smith, T., & Zhang, H.-M. (2020). Improvements of the Daily Optimum Interpolation Sea Surface Temperature (DOOIST) Version 2.1. [2001–2019]. NOAA National Centers for Environmental Information. https://doi.org/10.25921/RE9P-PT57

Humphreys, R. L. (2000). Otolith-based assessment of recruitment variation in a North Pacific seamount population of armorhead

Pseudopentaceros wheeleri. *Marine Ecology Progress Series*, *204*, 213–223. https://doi.org/10.3354/meps204213

Humphreys, R. L. (2008). Sources of information for evaluating the existence of vulnerable marine ecosystems (VMEs) on seamounts within the Southern Emperor-Northern Hawaiian Ridge. WP-08-003. https://repository.library.noaa.gov/view/noaa/15656

Humphreys, R. L., Crossler, M. A., & Rowland, C. M. (1993). Use of a monogenean gill parasite and feasibility of condition indices for identifying new recruits to a seamount population of armorhead, *Pseudopentaceros wheeleri* (Pentacerotidae). *Fishery Bulletin*, *91*, 455–463. PMID: https://www.semanticscholar.org/paper/Use-of-a-monogenean-gill-parasite-and-feasibility-a-Humphreys-Rowland/e0d1285599c8b9f313398492930499f4d0a70afa

Humphreys, R. L., Winans, G. A., & Tagami, D. T. (1989). Synonymy and life history of the North Pacific Pelagic Armorhead, *Pseudopentaceros wheeleri* Hardy (*Pisces*: Pentacerotidae). *Copeia*, *1*, 142–153. https://www.jstor.org/stable/1445615?seq=1#metadata_info_tab_contents. https://doi.org/10.2307/1445615

Johnson, Z. F., Chikamoto, Y., Wang, S.-Y., McPhaden, M. J., & Mochizuki, T. (2020). Pacific Decadal oscillation remotely forced by the equatorial Pacific and the Atlantic oceans. *Climate Dynamics*, *55*, 789–811. https://doi.org/10.1007/s00382-020-05295-2.pdf

Keister, J. E., di Lorenzo, E., Morgan, C. A., Combes, V., & Peterson, W. T. (2010). Zooplankton species composition is linked to ocean transport in the North California current. *Global Change Biology*, *17*(7), 2498–2511. https://doi.org/10.1111/j.1365-2486.2010.02383.x

Keyl, F., & Wolff, M. (2008). Environmental variability and fisheries: What can models do? *Reviews in Fish Biology and Fisheries*, *18*, 273–299. https://doi.org/10.1007/s11160-007-9075-5

Kiyota, M., Nishida, K., Murakami, C., & Yonezaki, S. (2016). History, biology, and conservation of Pacific Endemics 2. The North Pacific Armorhead, *Pentaceros wheeleri* (Hardy, 1983) (perciformes, pentacerotidae). *Pacific Science*, *70*(1), 1–20. https://doi.org/10.2984/70.1.1

Kiyota, M., Okuda, T., & Yonezaki, S. (2013). Stock status of the North Pacific armorhead (*Pseudopentaceros wheeleri*) and management proposal. SWG11/WP4/J, 11 pp. Available from North Pacific fisheries commission. 2F Hakuyo-Hall, Tokyo University of Marine Science and Technology, 4–5-7 Konan, Minato-ku, Tokyo 108–8477 JAPAN.

Lange, M., & van Sebille, E. (2017). Parcels v0.9: Prototyping a Lagrangian ocean analysis framework for the petascale age. *Geoscientific Model Development*, *10*, 4175–4186. https://doi.org/10.5194/gmd-10-4175-2017

Lanz, E., Lopez-Martinez, J., Nevarez-Martinez, M., & Dworak, J. A. (2009). Small pelagic fish catches in the Gulf of California associated with sea surface temperature and chlorophyll. CalCOFI Rep., 50. https://www.researchgate.net/publication/279558258_Small_pelagic_fish_catches_in_the_Gulf_of_California_associated_with_sea_surface_temperature_and_chlorophyll

Laurs, R. M., & Lynn, R. J. (1977). Seasonal migration of north pacific albacore, *Thunnus alalunga*, into North American coastal waters: Distribution, relative abundance and association with transition zone waters. *Fishery Bulletin*, *74*(4), 795–822. PMID: https://spo.nmfs.noaa.gov/sites/default/files/pdf-content/fishbull/laurs%20%281%29.pdf

Lee, Y. W., Megrey, B. A., & Macklin, S. A. (2009). Evaluating the performance of Gulf of Alaska walleye pollock (*Theragra chalcogramma*) recruitment forecasting models using a Monte Carlo resampling strategy. *Canadian Journal of Fisheries and Aquatic Sciences*, *66*, 367–381. https://doi.org/10.1139/F08-203

Lien, Y.-H., Su, N.-J., Sun, C.-L., Punt, A. E., Yeh, S.-Z., & DiNardo, G. (2014). Spatial and environmental determinants of the distribution of Striped Marlin (*Kajikia audax*) in the western and central North Pacific Ocean. *Environmental Biology of Fishes*, *97*, 267–276. https://doi.org/10.1007/s10641-013-0149-z

Litzow, M. A., Ciannelli, L., Puerta, P., Wettstein, J. J., Rykaczewski, R. R., & Opiekun, M. (2018). Non-stationary climate-salmon relationships in the Gulf of Alaska. *Proceedings of the Royal Society B: Biological Sciences*, *285*(1890), 20181855. https://doi.org/10.1098/rspb.2018.1855

Litzow, M. A., Hunsicker, M. E., Bond, N. A., Burke, B. J., Cunningham, C. J., Gosselin, J. L., Norton, E. L., Ward, E. J., & Zafor, S. G. (2020). The changing physical and ecological meanings of North Pacific ocean climate indices. *PNAS*, *117*(14), 7665–7671. https://doi.org/10.1073/pnas.1921266117

Lobel, P. S., & Robinson, A. R. (1986). Transport and entrapment of fish larvae by ocean mesoscale eddies and currents in Hawaiian waters. *Deep-Sea Research*, *33*(4), 483–500. https://www.sciencedirect.com/science/article/pii/0198014986901275. https://doi.org/10.1016/0198-0149(86)90127-5

Ludsin, S. A., DeVanna, K. M., & Smith, R. E. H. (2014). Physical-biological coupling and the challenge of understanding fish recruitment in freshwater lakes. *Canadian Journal of Fisheries and Aquatic Sciences*, *71*(4), 775–794. https://doi.org/10.1139/cjfas-2013-0512

Mantua, N. J., Hare, S., Zhang, Y., Wallace, J. M., & Francis, R. C. (1997). A Pacific Interdecadal climate oscillation with impacts on salmon production. *Bulletin of the American Meteorological Society*, *78*(6), 1069–1079. PMID: https://doi.org/10.1175/1520-0477(1997)078%3C1069:APICOW%3E2.0.CO;2

Mantua, N. J., & Hare, S. R. (2002). The Pacific decadal oscillation. *Journal of Oceanography*, *58*(1), 35–44. https://doi.org/10.1023/A:1015820616384

Mugo, R., Saitoh, S.-I., Nihira, A., & Kuroyama, T. (2010). Habitat characteristics of skipjack tuna (Katsuwonus pelamis) in the western North Pacific: A remote sensing perspective. *Fisheries Oceanography*, *19*(5), 382–396. https://doi.org/10.1111/j.1365-2419.2010.00552.x

Murakami, C., Yonezaki, S., Suyama, S., Nakagami, O., Okuda, T., & Kiyota, M. (2016). Early epipelagic life-history characteristics of the North Pacific armorhead *Pentaceros wheeleri*. *Fisheries Science*, *82*, 709–718. https://doi.org/10.1007/s12562-016-1002-z

National Center for Atmospheric Research. (2022). The climate data guide: North Pacific (NP) Index by Trenberth and Hurrell; monthly and winter. https://climatedataguide.ucar.edu/climate-data/north-pacific-np-index-trenberth-and-hurrell-monthly-and-winter

Newman, M., Alexander, M. A., Ault, T. R., Cobb, K. M., Deser, C., di Lorenzo, E., Mantua, N. J., Miller, A. J., Minobe, S., Nakamura, H., Schneider, N., Vimont, D. J., Phillips, A. S., Scott, J. D., & Smith, C. A. (2016). The Pacific decadal oscillation, revisited. *Journal of Climate*, *29*(12), 4399–4427. https://doi.org/10.1175/JCLI-D-15-0508.1

Nishida, K., Murakami, C., Yonezaki, S., Miyamotot, M., Okuda, T., & Kiyota, M. (2016). Prey use by three deep-sea fishes in the Emperor Seamount waters, North Pacific Ocean, as revealed by stomach contents and stable isotope analyses. *Environmental Biology of Fishes*, *99*(4), 335–349. https://doi.org/10.1007/s10641-16-0477-x

NOAA Climate Prediction Center. (2022a). Artic Oscillation (AO). https://origin.cpc.ncep.noaa.gov/products/precip/CWlink/daily_ao_index/ao.shtml.

NOAA Climate Prediction Center. (2022b). ONI_v5. https://origin.cpc.ncep.noaa.gov/products/analysis_monitoring/ensostuff/ONI_v5.php

NOAA National Centers for Environmental Information. (2022). Pacific Decadal Oscillation. https://www.ncdc.noaa.gov/teleconnections/pdo/

NOAA Physical Sciences Laboratory. (2022). Multivariate ENSO Index Version 2 (MEI.v2). https://psl.noaa.gov/enso/mei/

Norcross, B. L., & Shaw, R. F. (1984). Ocean and estuarine transport of fish eggs and larvae: A review. *Transactions of the American Fisheries Society*, *113*(2), 153–165. PMID: https://10.1577/1548-8659(1984)113<153:OAETOF>2.0.CO;2

NPFC. (2021). CMM 2021-05. Conservation and management measure for bottom fisheries and protection of vulnerable marine ecosystems in the Northwestern Pacific Ocean. https://www.npfc.int/cmm-2021-05-bottom-fisheries-and-protection-vmes-nw-pacific-ocean Accessed 25 August 2022.

NPFC. (2021). NPFC-2021-AR-annual summary footprint—Bottom fisheries. https://www.npfc.int/statistics

Olla, B. L., & Davis, M. W. (1990). Effects of physical factors on the vertical distribution of larval walleye pollock *Theragra chalcogramma* under controlled laboratory conditions. *Marine Ecology Progress Series*, *63*, 105–112. https://doi.org/10.3354/meps063105

O'Reilly, J. E., Maritorena, S., Mitchell, B. G., Siegel, D. A., Carder, K. L., Garver, S. A., Kahru, M., & McClain, C. (1998). Ocean color chlorophyll algorithms for SeaWiFS. *Journal of Geophysical Research*, *103*, 24937–24953. https://doi.org/10.1029/98JC02160

Otterson, G., & Loeng, H. (2000). Covariability in early growth and year-class strength of Barents Sea cod, haddock and herring: The environmental link. *ICES Journal of Marine Science*, *57*(2), 339–348. https://doi.org/10.1006/jmsc.1999.0529

Pattrick, P., Weidberg, N., Goschen, W. S., Jackson, J. H., McQuaid, C. D., & Porri, F. (2021). Larval fish assemblage structure at coastal fronts and the influence of environmental variability. *Frontiers in Ecology and Evolution*, *9*, 1–15. https://doi.org/10.3389/fevo.2021.684502/full

Pearcy, W. G. (1991). Biology of the transition region. In J. Wetherall (Ed.), *Biology, oceanography, and fisheries of the North Pacific transition zone and subarctic frontal zone* (pp. 39–59). NOAA Tech. Reo. NMFS 105.

Pécuchet, L., Nielsen, J. R., & Christensen, A. (2015). Impacts of the local environment on recruitment: A comparative study of North Sea and Baltic Sea fish stocks. *ICES Journal of Marine Science*, *72*(5), 1323–1335. https://doi.org/10.1093/icesjms/fsu220

Peterson, W. T., & Schwing, F. B. (2003). A new climate regime in northeast pacific ecosystems. *Geophysical Research Letters*, *30*(17). https://doi.org/10.1029/2003GL017528

Polovina, J. J., Howell, E., Kobayashi, D. R., & Seki, M. P. (2001). The transition zone chlorophyll front, a dynamic global feature defining migration and forage habitat for marine resources. *Progress in Oceanography*, *49*(1), 469–483. https://doi.org/10.1016/S0079-6611(01)00036-2

Polovina, J. J., Howell, E., Kobayashi, D. R., & Seki, M. P. (2017). The transition zone chlorophyll front updated: Advances from a decade of research. *Progress in Oceanography*, *150*, 79–85. https://doi.org/10.1016/j.pocean.2015.01.006

R Core Team. (2021). *R: A language and environment for statistical computing*. R Foundation for Statistical Computing. https://www.R-project.org/

Rio, M.-H., Mullet, S., & Picot, N. (2014). Beyond GOCE for the ocean circulation estimate: Synergetic use of altimetry, gravimetry, and in situ data provides new insight into geosrophic and Ekman currents. *Geophysical Research Letters*, *41*, 8918–8925. https://doi.org/10.1002/2014GL061773

Roden, G. I. (1984). Aspects of oceanic flow and thermohaline structure in the vicinity of seamounts. In R. N. Uchida, S. Hayasi, & G. W. Boehlert (Eds.), *Environment and resources of seamounts in the North Pacific* (pp. 3–12). NOAA Tech. Rep. NMFS 43. U.S. Dept of Comm. Washington, DC. https://www.cbd.int/doc/meetings/mar/ebsa-np-01/other/ebsa-np-01-submission-noaa-02-en.pdf

Rodionov, S. N., Bond, N. A., & Overland, J. E. (2007). The Aleutian low, storm stracks and winter climate variability in the Bering Sea. *Deep Sea Research Part II: Topical Studies in Oceanography*, *54*(23–26), 2560–2577. https://doi.org/10.1016/j.dsr2.2007.08.002

Saba, V. S., Friedrichs, M. A. M., Antoine, D., Armstrong, R. A., Asanuma, I., Behrenfeld, M. J., Ciotti, A. M., Dowell, M., Hoepffner, N., Hyde, K. J. W., Ishizaka, J., Kameda, T., Marra, J., Mélin, F., Morel, A., O'Reilly, J., Scardi, M., Smith, W. O. Jr., Smyth, T. J., … Westberry, T. K. (2011). An evaluation of ocean color model estimates of marin primary productivity in coastal and pelagic regions across the globe. *Biogeosciences*, *8*, 489–503. https://doi.org/10.5194/bg-8-489-2011

Sánchez-Velasco, L., Lavín, M. F., Jiménez-Rosenberg, G., Godínez, V. M., Santamaría-del-Angel, E., & Hernández-Becerril, D. U. (2013). Three-dimensional distribution of fish larvae in a cyclonic eddy in the Gulf of California during the summer. *Deep Sea Research Part 1: Oceanographic Research Papers*, *75*, 39–51. https://doi.org/10.1016/j.dsr.2013.01.009

Sasaki, T. (1986). Development and present status of Japanese trawl fisheries in the vicinity of seamounts. In R. N. Uchida, S. Hayashi, & G. W. Boehlert (Eds.), *Environment and resources of seamounts in the North Pacific* (pp. 21–30). NOAATech. Rep. NMFS 43. U.S. Dept. of Commerce. Washington, D.C. https://www.cbd.int/doc/meetings/mar/ebsa-np-01/other/ebsa-np-01-submission-noaa-02-en.pdf

Schilling, H. T., Everett, J. D., Smith, J. A., Stewart, J., Hughes, J. M., Roughan, M., Kerry, C., & Suthers, I. M. (2020). Multiple spawning events promote increased larval dispersal of a predatory fish in a western boundary current. *Fisheries Oceanography*, *20*, 309–323. https://doi.org/10.1111/fog.12473

Schwing, F. B., Jiang, J., & Mendelssohn, R. (2003). Coherency of multiscale abrupt changes between the NAO, NPI, and PDO. *Geophysical Research Letters*, *30*(7), 1–4. https://doi.org/10.1029/2002GL016535

Shaari, N. R., & Mustapha, M. A. (2018). Predicting potential *Rastrelliger kanagurta* fish habitat using MODIS satellite data and GIS modeling: A case study of exclusive economic zone, Malaysia. *Sains Malaysiana*, *47*(7), 1369–1378. https://doi.org/10.17576/JSM-2018-4707-03

Solanki, H. U., Mankodi, P. C., Dwivedi, R. M., & Nayak, S. R. (2008). Satellite observations of main oceanographic processes to identify ecological associations in the Northern Arabian Sea for fishery resources exploration. *Hydrobiologia*, *612*, 269–279. https://doi.org/10.1007/978-1-4020-9141-4_20

Solanki, H. U., Mankodi, P. C., Nayak, S. R., & Somvanshi, V. S. (2005). Evaluation of remote-sensing-based potential fishing zones (PFZs) forecast methodology. *Continental Shelf Research*, *25*(18), 2163–2173. https://doi.org/10.1016/j.csr.2005.08.025

Somerton, D. A., & Kikkawa, B. S. (1992). Population dynamics of pelagic armorhead *Pseudopentaceros wheeleri* on Southeast Hancock seamounts. *Fish. Bull. US*, *90*, 756–769. PMID: https://spo.nmfs.noaa.gov/sites/default/files/pdf-content/1992/904/somerton.pdf

Surry, A. M., & King, J. R. (2015). A new method for calculating ALPI: The Aleutian low pressure index. *Canadian Technical Report of Fisheries and Aquatic Sciences*, *3135*. PMID: v + 31 p. https://www.dfo-mpo.gc.ca/science/documents/data-donnees/climatology-climatologie/alpi-eng.txt

Swearer, S. E., Treml, E. A., & Shima, J. S. (2019). A review of biophysical models of marine larval dispersal. *Oceanography and Marine Biology: An Annual Review*, *57*, 325–356. https://doi.org/10.1201/9780429026379-7

Thompson, D. W. J., & Wallace, J. M. (2000). Annular modes in the extratropical circulation. Part 1: Month-to-month variability. *Journal of Climate*, *13*(5), 1000–1016. PMID: https://journals.ametsoc.org/view/journals/clim/13/5/15200442_2000_013_1000_amitec_2.0.co_2.xml?tab_body=fulltext-display

Trenberth, K. E., & Hurrell, J. W. (1994). Decadal atmosphere-ocean variations in the Pacific. *Climate Dynamics*, *9*, 303–319. https://doi.org/10.1007/BF00204745

Uchida, R. N., & Tagami, D. T. (1984). Groundfish fisheries and research in the vicinity of seamounts in the North Pacific Ocean. *Marine Fisheries Review*, *46*(2), 1–17.

Uchiyama, J. H., & Sampaga, J. D. (1990). Age estimation and composition of pelagic armorhead *Pseudopentaceros wheeleri* from the Hancock seamounts. *Fishery Bulletin*, *88*(1), 217–222. PMID: https://spo.nmfs.noaa.gov/content/age-estimation-and-composition-pelagic-armorhead-pseudopentaceros-wheeleri-hancock-seamounts

van Sebille, E., Griffies, S. M., Abernathey, R., Adams, T. P., Berloff, P., Biastoch, A., Blanke, B., Chassignet, E. P., Cheng, Y., Cotter, C. J., Deleersnijder, E., Döös, K., Drake, H. F., Drijfhout, S., Gary, S. F., Heemink, A. W., Kjellsson, J., Koszalka, I. M., Lange, M., … Zika, J. D. (2018). Lagrangian ocean analysis: Fundamentals and practices. *Ocean Modelling*, *121*, 49–75. https://doi.org/10.1016/j.ocemod.2017.11.008

Wallace, J. M., & Gutzler, D. S. (1981). Teleconnections in the geopotential height field during the northern hemisphere winter. *Monthly Weather*

Review, *109*(4), 784–812. PMID: https://doi.org/10.1175/1520%2D0493(1981)109%3C0784:TITGHF%3E2.0.CO;2

Wetherall, J. A., & Yong, M. Y. (1986). Problems in assessing the pelagic armorhead stock on the central North Pacific seamounts. In R. N. Uchida, et al. (Eds.), *Environment and resources of the seamounts in the North Pacific* (pp. 73–86). NOAA Tech. Rep. NMFS 43.

Wilson, J. R., Broitman, B. R., Caselle, J. E., & Wendt, D. E. (2008). Recruitment of coastal fishes and oceanographic variability in central California. *Estuarine, Coastal and Shelf Science*, *79*(3), 483–490. https://doi.org/10.1016/j.ecss.2008.05.001

Wolanki, E., & Hamner, W. M. (1988). Topographically controlled fronts in the ocean and their biological significance. *Science*, *241*, 4862. PMID: https://link.gale.com/apps/doc/A6504498/AONE?u=googlescholar&sid=bookmark-AONE&xid=941ce532

Wood, S. N. (2006). *Generalized additive models: An introduction with R*. Chapman & Hall. https://doi.org/10.1201/9781420010404

Wood, S. N. (2011). Fast stable restricted maximum likelihood and marginal likelihood estimation of semiparametric generalized linear models. *Journal of the Royal Statistical Society, Series B: Statistical Methodology*, *73*(1), 3–36. https://doi.org/10.1111/j.1467-9868.2010.00749.x

Yonezaki, S., Masujima, M., Okazaki, M., Miyamoto, M., Kiyota, M., & Okunishi, T. (2017). Relationship between the recruitment of North Pacific armorhead and marine environment: Results from particle tracking experiments for estimating the movement route and surrounding environment of the larvae. NPFC-2017-SSC NPA02-WP021.

Zainuddin, M. (2011). Skipjack tuna in relation to sea surface temperature and chlorophyll-a concentration of Bone Bay using remotely sensed satellite data. *Jurnal Ilmu Dan Teknologi Kelautan Tropis*, *3*(1), 82–90. https://doi.org/10.29244/jitkt.v3i1.7837

How to cite this article: Lavery, M. A. K., Rooper, C. N., Sowada, K., Fenske, K., Kulik, V., & Park, K. J. (2022). Effects of oceanography on North Pacific armorhead recruitment in the Emperor Seamounts. *Fisheries Oceanography*, 1–17. https://doi.org/10.1111/fog.12612